Contents lists available at ScienceDirect

Water Research

journal homepage: www.elsevier.com/locate/watres

Synergies of surface roughness and hydration on colloid detachment in saturated porous media: Column and atomic force microscopy studies

Tiantian Li [a], Chongyang Shen [a, *], Sen Wu [b], Chao Jin [c], Scott A. Bradford [d, **]

[a] Department of Soil and Water Sciences, China Agricultural University, Beijing, 100193, China
[b] School of Precision Instruments and Optoelectronics Engineering, Tianjin University, Tianjin, 300072, China
[c] School of Environmental Science and Engineering, Sun Yat-sen University, Guangzhou, Guangdong, 510006, China
[d] USDA, ARS, U.S. Salinity Laboratory, Riverside, CA, 92507-4617, United States

ARTICLE INFO

Article history:
Received 24 September 2019
Received in revised form
11 June 2020
Accepted 15 June 2020
Available online 20 June 2020

Keywords:
Colloids
Detachment
Hydration
Surface roughness
Porous media

ABSTRACT

Saturated column experiments were conducted to systematically examine the influence of hydration on the detachment of nano- and micro-sized latex colloids (35 nm and 1 μm, respectively) from sand. The colloids were attached on the sand in primary minima (PM) using high ionic strength (IS) NaCl solutions. The PM were predicted to be shallower and located farther from sand surfaces with increasing IS due to the hydration force. Consequently, a greater amount of colloid detachment occurred in deionized water when the colloids were initially deposited at a higher IS. Atomic force microscopy (AFM) examinations showed that both nanoscale protruding asperities and large wedge-like valleys existed on the sand surface. The influence of these surface features on the interaction energies/forces was modeled by approximating the roughness as cosinoidal waves and two intersecting half planes, respectively. The PM were deep and attachment was irreversible at concave regions for all ISs, even if the hydration force was included. Conversely, colloids were weakly attached at protruding asperities due to a reduced PM depth, and thus were responsible for the detachment upon IS reduction. The AFM examinations confirmed that the adhesive forces were enhanced and reduced (or even completely eliminated) at concave and convex locations of sand surfaces, respectively. These results have important implications for surface cleaning and prediction of the transport and fate of hazardous colloids and colloid-associated contaminants in subsurface environments.

1. Introduction

Attachment and detachment are two primary processes that inhibit and facilitate colloid transport in porous media, respectively (Ryan and Elimelech, 1996; Shen et al., 2012a). Attachment is defined as the adhesion of a colloid in solution onto a collector surface, and the opposite mechanism is referred to as detachment (Yao et al., 1971; Tosco et al., 2009). While colloid attachment has been examined extensively, much less attention has been given to colloid detachment (Crist et al., 2004; Fang et al., 2014; Pazmino et al., 2014; Molnar et al., 2015a; Bradford et al., 2015, 2017; Babakhani et al., 2017). Colloid detachment in porous media is desired for a variety of industrial and environmental processes. For example, membrane and deep bed filtration have been frequently used to remove colloids in water and wastewater (Batra et al., 2001; Miao et al., 2017). The filtration capacities of the membrane and deep bed decrease with increasing colloid attachment on these surfaces. Therefore, periodic detachment of colloids from these surfaces is critical to regenerating membranes and filter beds. Although engineered colloids such as nanoscale zero-valent iron have been shown to be very effective to remove contaminants from water (Shi et al., 2018; Chen et al., 2019; Tian et al., 2019), the application of these nanomaterials for *in-situ* soil remediation is very limited because they are readily attached to soil surfaces (Kang et al., 2016; Song et al., 2019). Therefore, understanding the mechanisms that control the detachment of nanomaterials from soil surfaces is critical to enhancing their mobilities and increasing

* Corresponding author.
** Corresponding author.
E-mail addresses: chongyang.shen@cau.edu.cn (C. Shen), Scott.Bradford@ars.usda.gov (S.A. Bradford).

https://doi.org/10.1016/j.watres.2020.116068
0043-1354/

efficiencies for *in-situ* soil and groundwater remediation.

Detachment of a colloid from a collector surface occurs when the adhesive force/torque that acts on the colloid is overcome by applied forces/torques from hydrodynamic shear and/or Brownian diffusion (Bergendahl and Grasso, 2000; Bedrikovetsky et al., 2011; Trauscht et al., 2015; Bradford et al., 2017). The adhesive force mainly arises from the various colloidal interactions between the colloid and the surface (Elimelech and O'Melia, 1990). van der Waals (VDW) attraction and electrostatic double-layer (DL) interaction are long-range colloidal interaction forces, which can be quantitatively described by the classic Derjaguin-Landau-Verwey-Overbeek (DLVO) theory (Verwey and Overbeek, 1948; Ryan and Elimelech, 1996). When the separation distance between the colloid and surface is within a few nanometers (e.g., <4 nm), short-range repulsive forces emerge, which can dominate the colloid-surface interaction (Ohki and Ohshima, 1999; Manciu and Ruckenstein, 2001; Grasso et al., 2002; Liang et al., 2007; Israelachvili, 2010). Colloid detachment cannot occur if the short-range repulsive forces are absent because colloids are predicted to be immobilized in deep primary energy wells, due to the dominance of VDW attraction over DL energy at small separation distances (Hahn and O'Melia, 2004; Hahn et al., 2004).

Hydration or structural force is a typical short-range repulsive force which accounts for the energy needed to dehydrate interacting surfaces containing ionic or polar species in aqueous solution (Ruckenstein and Manciu, 2003; Leng, 2012). Direct measurements using a force apparatus (Israelachvili and Pashley, 1983) showed that the hydration force is extremely strong at small separation distances, which can prevent the interacting surfaces from approaching any closer than 0.5–0.6 nm (i.e., the thickness of two water molecules) (Israelachvili and Wennerstrom, 1996; Israelachvili, 2010; Anand et al., 2016). The hydration force decays very rapidly with increasing separation distance (i.e., in an exponential manner) (Israelachvili and Wennerstrom, 1996; Israelachvili, 2010). In addition to the separation distance, the hydration force is highly dependent on the hydrophilicity of the interacting surfaces and solution chemistry such as hydrated cations, pH, and ionic strength (IS) (Pashley and Israelachvili, 1984; Israelachvili and Wennerstrom, 1996; Molina-Bolívar and Ortega-Vinuesa, 1999; Molina-Bolıvar et al., 2001; Anand et al., 2016). For example, various studies (Elimelech, 1990; Molina-Bolívar and Ortega-Vinuesa, 1999; Manciu and Ruckenstein, 2001; Miao et al., 2015, 2017) showed that when the concentration of an electrolyte solution exceeded a critical value, the repulsive hydration force could alter the interaction between surfaces. Pashley (1981, 1982) and Miao et al. (2015) experimentally showed that the hydration force altered the interaction energy when the electrolyte concentration was 10 mM for NaCl; e.g., the critical value.

Manciu and Ruckenstein (2001, 2004) and Song et al. (2005) showed that the strong repulsion due to hydration can keep hydrophilic colloids (e.g., silica and latex particles) monodispersed in high electrolyte solutions, even though classic DLVO theory predicts coagulation under these chemical conditions. This is due to sorption of hydrated cations (Na^+ or Ca^{2+}) onto the particle/water interface, which increased the volume of hydration layers and thus inhibited particle aggregation (Song et al., 2005). Miao et al. (2015, 2017) showed that hydration forces can decrease the fouling of membranes by negatively charged protein colloids (i.e., bovine serum albumin). Elimelech (1990) conducted column experiments to examine the attachment of latex colloids in glass-bead porous media and showed that repulsive hydration forces caused an anomalous decrease of attachment efficiencies with increasing electrolyte concentration at high IS. Even though the repulsive hydration force has been identified to reduce aggregation and attachment, its influence on colloid detachment has not been investigated to date. The mechanisms that control the detachment of colloids from collector surfaces could be very complex due to the coupling of repulsive hydration forces with surface heterogeneity (e.g., nanoscale roughness). Surface roughness has been indicated to play an important role in both colloid attachment and detachment (Bradford and Torkzaban, 2015; Bradford et al., 2017; Rasmuson et al., 2019).

Saturated column experiments were conducted to systematically examine effects from a repulsive hydration force on the detachment of nano- and micro-sized colloids (denoted as NCs and MCs, respectively) from sand surfaces that contains heterogeneities. The colloids were first attached in primary minima on sand (without colloid breakthrough) using different electrolyte concentrations at a high IS. More colloids were attached with weak adhesions at a higher IS due to an increased repulsive hydration force, and these colloids were susceptible to detachment when the IS was reduced to deionized (DI) water. The mechanisms controlling the detachment of colloids from rough surfaces by the presence of repulsive hydration forces were interpreted by calculating DLVO energies using the surface element integration (SEI) technique and determining adhesive forces via atomic force microscopy (AFM) examinations. The findings in this study advanced our understanding about mechanisms controlling colloid detachment in natural and engineered systems, which has important implication to surface cleaning, water treatment and prediction of colloid-facilitated contaminant transport in subsurface environments.

2. Materials and methods

2.1. Colloidal particles and porous media

White, spherical, carboxylate-modified polystyrene latex particles with sizes of 35 nm and 1 μm (Fisher Scientific, Inc.) were used as model NCs and MCs, respectively. Both colloids are hydrophilic with a density of 1.055 g/cm^3 (reported by the manufacturer). Colloidal influent suspensions for column transport experiments were prepared by diluting the stock colloid suspensions using NaCl solution at different ISs (0.05, 0.1, 0.2, and 0.5 M) to achieve a colloid concentration of 20 mg/L. The pH of the colloidal influent suspensions was adjusted to 7 by addition of 1 mM $NaHCO_3$. Colloid concentrations of the effluent suspensions from the column experiments were measured using a UV–vis spectrophotometry (DU Series 800, Beckman Instruments, Inc., Fullerton, California) at a wavelength of 225 nm and 430 nm for the NCs and MCs, respectively.

Quartz sand, purchased from Sigma-Aldrich (St. Louis, Missouri), with sizes ranging from 300 to 355 μm was used to pack the columns. The method of Zhuang et al. (2005) was used to extensively remove metal oxides and other impurities on this sand. The cleaned sand surfaces were examined using a Hitachi S4300 scanning electron microscope (SEM) (Hitachi Co., Tokyo, Japan). The SEM measurements show that the sand surfaces were very rough [see Supplementary Material (SM) Fig. S1]. The roughness morphology was similar to those in previous studies (Alshibli and Alsaleh, 2004; Wang et al., 2016a).

Sizes of the NCs and MCs and zeta potentials of the colloids and sand were determined in NaCl solutions at selected ISs using a Zetasizer Nano ZS (Malvern Instruments Ltd., Southborough, Massachusetts). A method from previous studies (Tufenkji and Elimelech, 2004, 2005; Zhou et al., 2011; Li et al., 2017) was used to measure zeta potentials of sand. Briefly, the cleaned sand was sonicated for 5 min in an electrolyte solution of interest and samples of the supernatant were then taken for zeta potential measurements.

2.2. Column transport experiments

Acrylic columns that are 1.8-cm in inner diameter and 9-cm long were used for column transport experiments. The cleaned sand was incrementally wet-packed in the column, and gently vibrated to minimize any layering and air entrapment. The porosities of packed sand beds (φ) were determined to be ~0.36 using$\phi = 1 - m/(\rho V)$, where m is the dry mass of packed sand, V the is volume of the column, and ρ is the density of sand grains (taken as 2.65 g/cm^3).

All column transport experiments were done at an approach velocity of 4×10^{-5} m/s (0.24 cm/min). Background NaCl solution was first injected upward into a column for at least 20 pore volumes (PVs) to equilibrate the solution chemistry of the system. Similar to previous studies (Hahn and O'Melia, 2004; Hahn et al., 2004; Li et al., 2017), a three-step procedure was then used to examine the attachment and detachment of colloids. Briefly, ~5 PVs of colloid suspension was introduced to the packed column to allow the colloids to be attached at a given IS (0.05, 0.1, 0.2 or 0.5 M) (phase 1), followed by elution with colloid-free electrolyte solution to displace unattached colloids in pore water (phase 2), and finally elution with DI water to detach the colloids that were initially attached in phase 1 (phase 3). Note that the colloids that were loosely associated with collectors or in low flow regions via secondary minimum energy association could also be released during phase 2 and 3 (Johnson et al., 2018). The fraction of reentrained colloids (FRA) was calculated as FRA $= M_3/(1 - M_{12})$, where M_{12} is the fraction of colloids recovered from phases 1 and 2 and M_3 is the recovered fraction during phase 3.

For selected transport experiments, two additional phases were initiated following completion of phase 3. Specifically, the hydration force was increased by increasing the solution IS using ~58 PVs of 1 M colloid-free NaCl electrolyte solution at pH 7 during phase 4. The column was subsequently flushed with DI water during phase 5 to examine whether additional colloid detachment could be achieved. Blank experiments were conducted using colloid-free background electrolyte solution instead of colloid suspension during phase 1. These blank experiments showed that negligible colloidal impurities were detached from the sand during phases 1–5. These results confirmed that the method of Zhuang et al. (2005) was very effective in removing colloidal impurities from the sand.

2.3. Atomic force microscopy measurements

In addition to the aforementioned SEM measurements, the sand surface roughness was also characterized by an AFM (Dimension Icon, Bruker Co., Karlsruhe, Germany) holding a regular silicon nitride (Si_3N_4) tip (NP-10, Bruker) with a nominal spring constant of 0.06 N/m. Specifically, the sand grains were fixed on a glass slide using UV glue (solidification by UV light), and the grain surfaces were imaged using contact-mode in air. The scanned area of each measurement was 10 × 10 μm. Fig. S2 in the SM shows a typical AFM image of the sand surface and measured values of roughness parameters including mean (m), average roughness (R_a), root-mean-square roughness (R_q), maximum roughness (R_m), and surface area difference (SAD).

Force curves were determined by interacting sand surfaces with silicon ball probes (SICON–B35, Appnano) of a diameter of 35 nm and a nominal spring constant of 0.29 N/m under the chemical conditions used in the column experiments via contact mode. Both convex and concave locations on sand surfaces were measured for each chemical condition. Adhesion maps were obtained via force volume mode using the method of Vadillo-Rodriguez and Logan (2006). Briefly, retraction force curves were obtained in 16 × 16 arrays over scan areas of 2 × 2 μm. The maximum negative force (i.e., adhesion force) during tip retraction for each force curve of a scan area as a function of the x-y location was plotted to obtain the adhesion maps. Surface heights at the x-y locations where the adhesions were measured were also recorded to obtain height maps. Details about the procedures for the measurements of force curves and adhesion/height maps were shown in the SM.

2.4. Calculation of DLVO interaction energies and forces

Both the SEM image in SM Fig. S1 and the AFM image in SM Fig. S2 show that the sand surfaces are very rough. Nanoscale protruding asperities and microscale wedge-like concave asperities were densely and sparsely distributed over the surface, respectively. To determine the influence of these two main roughness features on colloid attachment and detachment, the interaction energies between a colloid and these features were calculated. The nanoscale protruding asperities and wedge-like concave asperities were represented as cosinoidal waves and two intersecting half planes, respectively (cf., Fig. 1). The cosinoidal surface was described using the following expression (Zhao et al., 2016; Hong et al., 2017):

$$Z(x,y) = p_x \cos(\pi x / 2w_x) + p_y \cos(\pi y / 2w_y) \quad (1)$$

where the terms (p_x, p_y) and ($\pi/2w_x$, $\pi/2w_y$) are the scaled amplitudes and frequencies of the asperities on a rough surface in x and y directions, respectively. A planar surface can be represented using Eq. (1) by setting $p_x = 0$ and $p_y = 0$.

The SEI technique, developed by Bhattacharjee and Elimelech (1997) and Bhattacharjee et al. (1998), was used to calculate the interaction energies for a colloid interacting with the cosinoidal surface. Briefly, the colloid surface was discretized into small area elements (dS). The total interaction energy (U) was obtained by summing the differential interaction energy (E) between each area element dS on the colloid surface and the corresponding area element dS' on the cosinoidal surface. The differential interaction energy was considered as the sum of VDW attraction, DL interaction, Born (BR), and hydration (HR) interactions (Mahmood et al., 2001; Pazmino et al., 2014; Bradford et al., 2017). The expressions used to calculate E^{VDW}, E^{DL}, E^{BR}, and E^{HR} were shown in SM Table S1. Note that the equation of Molina-Bolivar and Ortega-Vinuesa (1999) was used to calculate E^{HR}, which considers that the hydration interaction energy is proportional to the electrolyte concentration or IS. The calculated interaction energies were made dimensionless by dividing by the product of the Boltzmann constant (k) and the absolute temperature (T).

For the interaction of the colloid with the two half planes, the interaction force was calculated instead of the energy because it is more convenient for interpreting colloid mobilization within the concave surface (Li et al., 2017). The expressions in SM Table S2 were used to determine separation distances between a colloid and the two half planes. The SEI technique was used to calculate the interaction force between a colloid and a half plane. The total interaction force between the colloid and two intersecting half planes was obtained as the vector sum of the two force components that act on the colloid. Detailed procedures for calculating the interaction energies or forces between the colloid and the two roughness features have been shown in the SM.

3. Results and discussion

3.1. Characteristics of colloids and collectors

SM Table S3 shows measured zeta potentials of the NCs, MCs, and sand in electrolyte solutions that were used in column experiments. The zeta potential values were negative at pH 7 for all

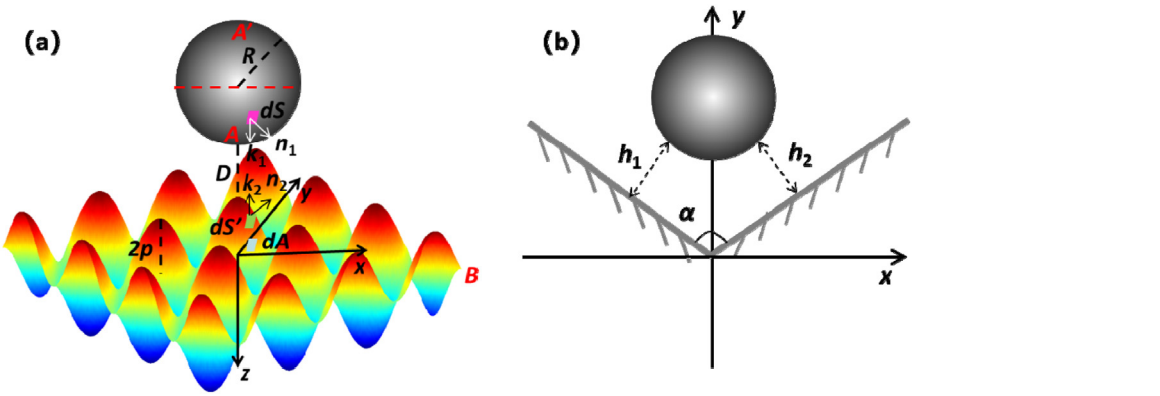

Fig. 1. Schematic illustration of a spherical colloid interacting with (a) a cosinoidal surface and (b) two intersecting half planes. dS is differential area element on the colloid and dS' is the corresponding area element on the cosinoidal surface; dA is the projected area of dS or dS' on the x-y plane; D is separation distance between the colloid and cosinoidal surface; n_1 and n_2 is units outward normal to the colloid and cosinoidal surfaces, respectively; k_1 and k_2 is unit vector directed towards the positive and negative z-axis, respectively; h_1 or h_2 is separation distance between the colloid and a half plane; α is angle between the two intercepting half planes.

considered solution ISs. Zeta potentials only reflect the average electrokinetic charge of the entire surface of the colloids and sand. Consequently, the net negative zeta potential does not reflect local charge variations (Elimelech et al., 2000). While the method of Zhuang et al. (2005) was used to extensively remove colloidal and chemical impurities from the sand surfaces in this study, the influence of surface charge heterogeneity on the attachment and detachment of colloids on/from the treated sand surfaces could still exist. This is because charge heterogeneity could arise, for example, from impurities or substitutions within mineral matrices that are exposed on the surface even after the removal of surface coating (Johnson et al., 2011). Previous theoretical and experimental studies (Santore and Kozlova, 2007; Shen et al., 2013, 2020; Pazmino et al., 2014; Trauscht et al., 2015) showed that surface charge heterogeneity can play a significant role on colloid attachment once the sizes or densities of the charge heterogeneities were larger than a critical value (which changes with system conditions such as IS). In these cases, the repulsive energy barriers were reduced to be comparable to the average kinetic energy of a colloid (i.e., 1.5 kT) or even completely disappeared, causing colloid attachment in primary minima. The value of zeta potential was less negative at higher IS, as frequently observed for the latex colloids and sand in the literature (Torkzaban and Bradford, 2016; Xu et al., 2016; Li et al., 2017).

As shown in SM Table S3, the sizes of the MCs and NCs in DI water were comparable to those in NaCl electrolyte solutions with IS $\leq$ 0.2 M, indicating that aggregation was insignificant at these ISs. This is because the carboxylate-modified polystyrene latex particles are stable in univalent salt solutions as reported by the manufacturer. When the IS was increased to 0.5 M, there was an evident increase of the MC size. Hence, a certain degree of aggregation occurred at this high IS for this large colloid.

3.2. Colloid attachment

Fig. 2 presents NC and MC breakthrough curves in sand when the solution IS ranged from 0.05 M to 0.5 M. Complete deposition (i.e., $C/C_0 = 0$, C and C_0 are effluent and influent concentration of colloids, respectively) occurred during phase 1 for NCs at all ISs and for MCs at IS $\geq$ 0.1 M. This indicates that all colloids were favorably attached in primary minima under these conditions. Using the correlation equation of Tufenkji and Elimelech (2004), the calculated single collector contact efficiency was 0.01 for the MC. The determined value of C/C_0 corresponding to attachment efficiency of unity was 0.1 for our column conditions via the expression of Logan et al. (1995a). This value was larger than those in phase 1 of Fig. 2, which verifies the favorable attachment in primary minima. Interaction energy calculations (see SM Fig. S3 and SM Table S4) cannot explain the favorable attachment in primary minima if the sand surface was assumed to be planar. Specifically, the calculations showed that repulsive energy barriers existed at IS $\leq$ 0.1 M for the NC and at IS $\leq$ 0.2 M for the MC. These energy barriers reduce the probability for attachment to occur when colloids strike the sand surfaces (Ryan and Elimelech, 1996); i.e., the attachment efficiency in colloid filtration theory is $\ll$1. Particularly, the calculated maximum energy barrier U_{max} was 10.7 kT at 0.05 M for the NC and 239.4 kT at 0.1 M for the MC. These values are significantly larger than the average kinetic energy of a colloid, which essentially inhibit attachment of any colloids in the primary minima. Note that if the hydration repulsion was included, the values of U_{max} were slightly increased (see SM Table S4), which further prevented the attachment in a primary minimum. However, both the NCs and MCs were completely attached under these chemical conditions.

Both SEM (SM Fig. S1) and AFM (SM Fig. S2) examinations show that the sand surfaces were very rough and exhibited densely distributed nanoscale protruding asperities and large wedge-like depressions. Surface roughness has been widely recognized as a major cause of the aforementioned discrepancies between the theoretical calculations and experimental observations (Zou et al., 2015; Bradford et al., 2017, 2018; Li et al., 2017; Kananizadeh et al., 2019). SM Tables S5 and S6 present calculated values of U_{max} for a cosinoidal surface with different values of w and p/w ($p = p_x = p_y$, $w = w_x = w_y$) interacting with the NC and MC at different ISs, respectively. The presence of nanoscale cosinoidal protrusions reduces the repulsive energy barrier, and accordingly increases colloid attachment in primary minima. For example, although the value of U_{max} was larger than 200 kT for the MC-planar surface interaction at 0.1 M, the energy barrier disappears between the MC and cosinoidal surfaces when $w = 10$ nm. Therefore, the MC is favorably attached at primary minima atop of protruding asperities. Notably, although the primary minimum depths are also reduced for the MC at 0.1 M with $w = 10$ nm, they are still significantly larger than the average kinetic energy of a colloid (e.g., 14.48 kT and 8.96 kT for $p/w = 0.5$ and $p/w = 1$, respectively). Thus, colloids can be maintained at the energy wells. The reduction of the energy barrier is more significant for larger value of p/w, which means that sharper asperities (i.e., smaller surface curvature) are more favorable for colloid attachment in primary minima. Similar findings have also been obtained for the interaction energy between a colloid and a rough surface modeled as a planar surface

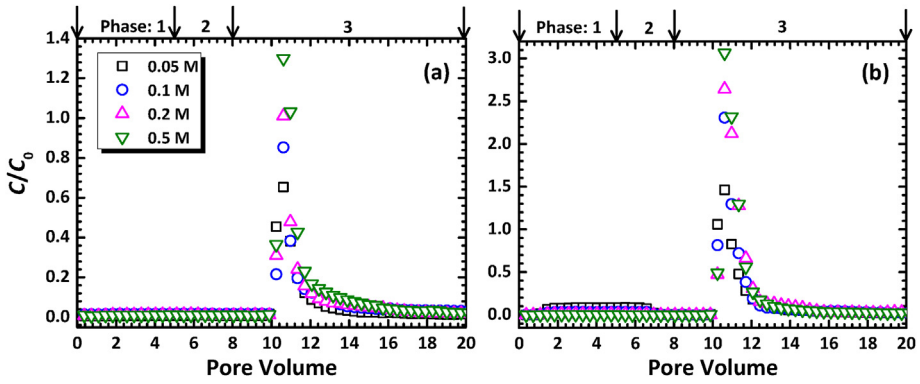

Fig. 2. Breakthrough curves for transport of the (a) NC and (b) MC in sand. Phase 1, attachment of the colloids at different ISs; Phase 2, elution with background electrolyte solution; Phase 3, elution with DI water.

carrying a hemispheroidal asperity (Shen et al., 2015).

If the charge heterogeneity is coupled with the physical protruding asperities, the repulsive energy barrier can be further reduced, causing an increase of attachment in primary minima (Shen et al., 2018, 2020; Rasmuson et al., 219; VanNess et al., 2019). For example, while the values of U_{max} are significant for the MC interacting with a cosinoidal surface at 0.05 M for $w = 30$ (28.54 and 14.06 kT for $p/w = 0.5$ and $p/w = 1$, respectively), the repulsive energy barrier disappears if the cosinoidal surface is assumed to be positively charged (zeta potential was taken to be 24 mV for calculations at 0.05 M). Therefore, the MCs were favorable to be attached on the sand surfaces with positively charged cosinoidal protrusions via primary minimum association. The charge heterogeneity could also solely result in attachment in primary minima provided that its size or distribution density is large enough to eliminate the repulsive energy barrier or reduce it to be comparable to the average kinetic energy of a colloid (Pazmino et al., 2014; Trauscht et al., 2015; Shen et al., 2020). In addition to the protruding asperities, the interaction force maps in SM Figs. S4 and S5 show that attachment in a primary minimum can also be increased in concave areas when repulsive force barriers are reduced or even disappear in the region close to the vertex of the depressions. The SEM examinations in SM Fig. S6 showed that the colloids were attached on protruding asperities and particularly concave locations of the sand surfaces. Notably, the aggregation of MCs in solution at 0.5 M (see the size measurements in SM Table S3) does not significantly influence the interaction energy because it is mainly determined by the interaction between the primary particles of aggregates and the surface (Lin and Wiesner, 2012). However, colloid aggregation can enhance retention by increasing sedimentation and straining at IS of 0.5 M (Solovitch et al., 2010).

Minor amounts of MCs were detected in the effluent in phase 1 when the solution IS equaled 0.05 and 0.1 M. The breakthrough was slightly more significant at 0.05 M than at 0.1 M. This is because of the existence of a critical IS, above which the protruding asperities can completely eliminate the repulsive energy barrier (see SM Tables S5 and S6). The critical IS value is smaller for sharper asperities (Wang et al., 2019). In addition, the size or density of a charge heterogeneity that can result in successful attachment is smaller at a higher IS (Shen et al., 2013). Hence, reducing solution IS can decrease the fraction of the sand surface where the repulsive energy barrier is eliminated. Consequently, a smaller fraction of colloids striking the surface will be successful in attachment when IS $\leq$ 0.1 M. Indeed, Li et al. (2017), through SEM examinations, showed that the colloids were uniformly attached on sand surfaces at high ISs and less attachments occurred at protruding asperities at a lower IS when sand was extensively treated to remove charge heterogeneity (the same treatment as used in this study). Complete attachment still occurred for the NC at the low ISs because the critical IS decreases with the decreasing colloid size (see SM Tables S5 and S6).

3.3. Colloid detachment

In phase 2 of Fig. 2, the columns were flushed with colloid-free NaCl electrolyte solutions to elute the unattached colloids in pore water. No colloids were detected during phase 2 when complete deposition occurred in phase 1. This illustrates that all injected colloids were rapidly attached. The colloidal concentration decreased from a very small value during phase 1 to zero in phase 2 at ISs of 0.05 and 0.1 M for the MCs. The unattached colloids in pore water were displaced out of the columns in this phase. The colloids that were loosely associated with shallow primary and secondary minima may also be reentrained from energy wells (Wang et al., 2016b; Hilpert et al., 2017). However, no tails existed in the breakthrough curves of phase 2, which implies that the reentrainment from shallow energy wells by Brownian diffusion and hydrodynamic drag was minor (Shen et al., 2007; Molnar et al., 2015). This is expected because the reentrainment from shallow energy wells mainly occurred when the colloids were initially attached at low ISs on relatively smooth surfaces (Kuznar and Elimelech, 2007; Shen et al., 2012b).

In phase 3 of Fig. 2, detachment of colloids occurred when the solution IS was decreased by flushing the columns with DI water. Interaction energy calculations showed that the depths of primary force minima (ΔF) are deep at concave locations at all solution ISs (cf., SM Fig. S7). Therefore, detached colloids should not be from concave locations on sand surfaces. Similarly, Rasmuson et al. (2019) showed that multiple interactions among asperities decrease detachment of colloids from rough silica surfaces. The SEM images in SM Fig. S6 confirms that colloids attached at concave locations were irreversibly retained when the solution IS was reduced, in agreement with the observations in Li et al. (2017). In contrast, interaction energy calculations in SM Tables S5 and S6 showed that the presence of protruding asperities can significantly reduce the primary minimum depth (ΔU) or detachment energy barrier. These interaction energy calculations are consistent with AFM examinations in Fig. 3 which shows that adhesion was enhanced and reduced at concave and convex locations, respectively. The adhesions can even disappear at convex locations, causing a repulsive interaction force (i.e., positive value of force) at all separation distances (e.g., SM Figs. S8a and S8d). The absence of adhesion is due to a monotonic decrease of the interaction energy with increasing separation distance (i.e., no primary energy well in an interaction energy curve). This is because the

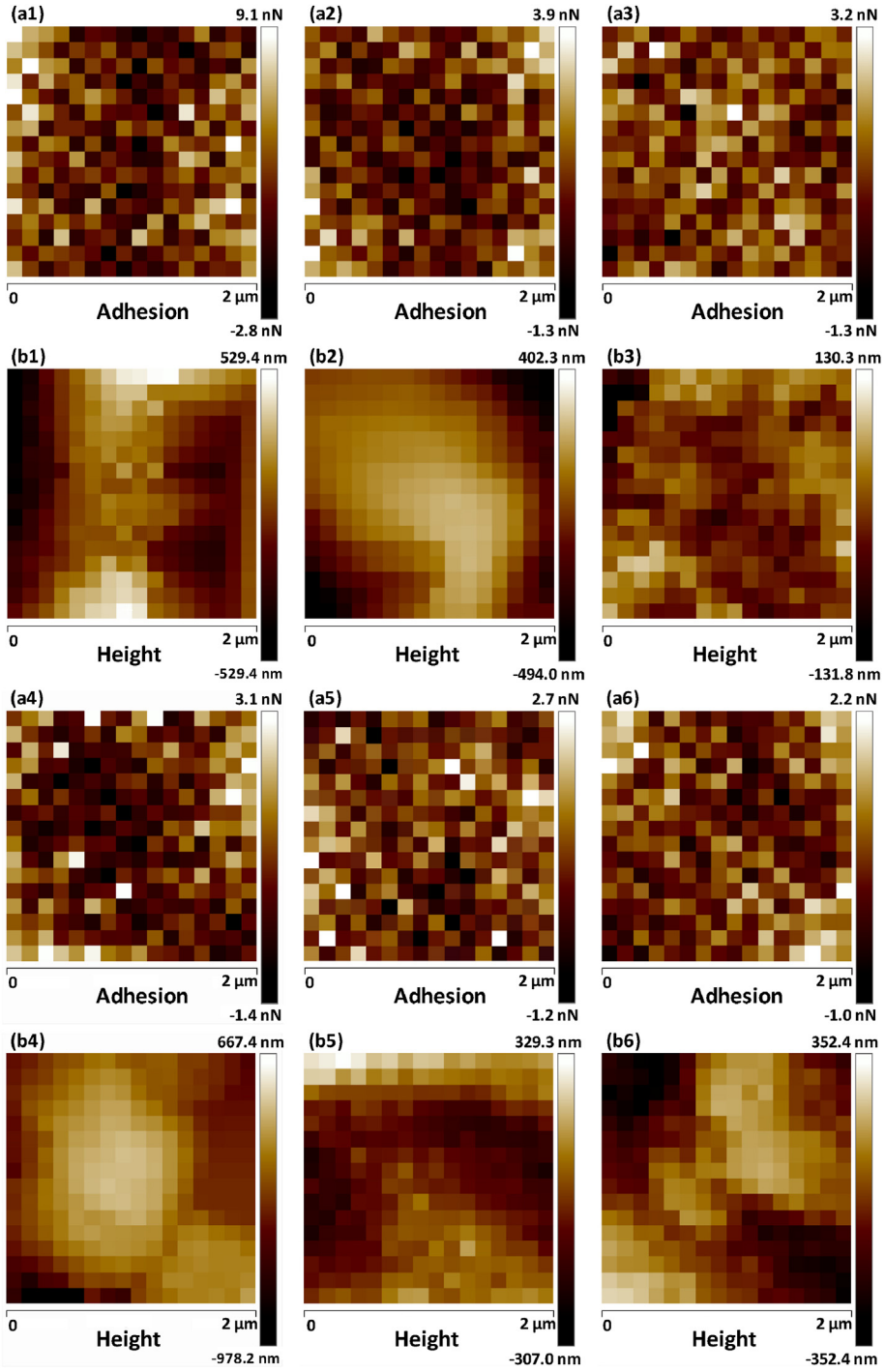

Fig. 3. Representative (a) adhesion maps and (b) corresponding height maps obtained using a silicon nitrite AFM tip on sand surfaces at different ISs (1, DI water; 2, 0.05 M; 3, 0.1 M; 4, 0.2 M; 5, 0.5 M; 6, 1 M). Positive and negative values indicate attractive and repulsive forces in (a), respectively. Positive and negative values indicate convex and concave areas in (b), respectively. (For interpretation of the references to colour in this figure legend, the reader is referred to the Web version of this article.)

shallow primary minimum between a colloid and a nanoscale protruding asperity is eliminated by the repulsive interaction energy from the bulk collector surface (Shen et al., 2012b, 2015, 2018). Therefore, colloids attached at convex locations will be detached by a reduction of solution IS if the forces that act on the colloids change from attractive to repulsive or if the attraction is small enough be overcome by hydrodynamic shear or Brownian diffusion. Yu et al. (2014) showed that protruding asperities (cuboid pillars or pits) on surfaces (silicon wafers) can reduce particle attachment even under favorable conditions (i.e., in the absence of repulsive energy barriers). The detachment of colloids from protruding asperities was confirmed by the SEM examinations shown in SM Fig. S6. Note that if the nanoscale protruding asperities also exhibit significant charge heterogeneity, the colloid could still attach atop the protruding asperities due to an increase of attraction by the charge heterogeneity.

While surface charge heterogeneity could significantly assist colloid attachment, it has little influence on colloid detachment compared to surface roughness when they co-exist on a surface

(Bradford and Torkzaban, 2015; VanNess et al., 2019). In fact, Shen et al. (2013) showed that surface charge heterogeneity increases the irreversibility of colloid attachment by increasing primary minimum depth. For example, the NC that was attached on the cosinoidal surface at 0.5 M with $w = 1$ and $w/p = 0.5$ at primary minimum (6.84 kT) could be detached upon reduction of solution IS to be lower than 0.1 M (primary minimum depth<0.84 kT). The attachment become irreversible to IS reduction if the cosinoidal surface is positively charged because the primary minimum depth is significant at all solution ISs (>10 kT). VanNess et al. (2019) showed that the detachment of colloids attached on charge heterogeneities of surfaces could occur even without physical protruding asperities if steric repulsion was included. However, steric repulsion arises from polymer and/or surfactant coatings on surfaces (Grasso et al., 2012), which were absent in our experimental systems. Consequently, detachment due to the coupled influence of surface charge heterogeneity and steric repulsion should be minor in our study.

Fig. 4 and SM Table S7 present calculated values of FRA for NC and MC at the solution IS when the colloids were attached (phase 1). The value of FRA was larger for the MC than the NC at a given IS. Similarly, Pazmino et al. (2014) showed that larger colloids were more susceptible to release when the IS was reduced. This is likely because the smaller size of the NC allows them to more readily approach [as shown by the trajectory simulations of Ron et al. (2019)] and then irreversibly attach at concave locations (see SM Fig. S6). Due to a similar reason, Rasmuson et al. (2019) showed that it was harder to detach colloids from surfaces with larger physical asperities by increasing flow velocity. It has to be noted that the complete deposition in phase 1 of Fig. 2 indicates that favorable attachment in primary minima was the main retention mechanism for the NC and MC due to use of high solution ISs, as mentioned previously. However, it is possible that a minor fraction of NC or MC was still attached at secondary minima in low flow regions (e.g., concave locations and grain-grain contacts) (Johnson et al., 2007; Molnar et al., 2015b). The MC was more favorably attached at secondary minimum than NC due to an increase of secondary minimum depth with colloid size (Hahn and O'Melia, 2004; Hahn et al., 2004). This could also be a reason for the larger value of FRA for the MC since the secondary minimum attachment is completely reversible in response to reduction of solution IS.

The value of FRA increased with increasing solution IS for both colloids. One possible explanation for the observation is that increasing IS increased repulsive hydration force (SM Fig. S9), causing the primary minima to be shallower and located farther from the protruding asperities (see Fig. 5a). When DI water was introduced to quickly reduce the IS, the hydrated cations may remain in the gaps between colloids and protruding asperity tips due to limited diffusion (Bradford and Kim, 2010), causing the colloids to be still located at the enlarged separation distances (see Fig. 5b). In contrast, the concentrations of salts in areas between the colloids and bulk sand surfaces could be rapidly decreased, resulting in an increase of DL repulsion. Colloids that were initially weakly attached at larger separation distances due to elevated hydration repulsion at higher IS are more susceptible to detachment with an IS reduction (Elimelech, 1990; Miao et al., 2015, 2017). Indeed, comparison of the adhesion maps with the height maps in Fig. 3 show that the maximum value of adhesion was smaller at higher IS for a rough surface. This confirms that more weak attachment sites were present at a higher IS. Fig. 5c illustrates that the colloids remain attached atop the asperities in DI water if the hydration cations are displaced and the hydration repulsion disappears. Therefore, colloids can be detached from these asperities only when they were initially attached at high ISs, causing an increase in FRA with increasing solution IS. Note that the high value of FRA for MCs when the IS = 0.5 M may also be due to disaggregation when the IS was reduced.

In addition to the aforementioned size measurements to show the aggregation of MCs at 0.5 M, the half-time of aggregation $T_{1/2}$ was determined for the MCs at this high IS to further testify that the MCs could be deposited as aggregates (Logan et al., 1995b). The expression developed by Szilagyi et al. (2014) for calculating the value of $T_{1/2}$ is $T_{1/2} = 2/(k_s N_0)$, where N_0 is initial particle concentration and k_s is rate coefficient of aggregation. When the repulsive energy between the MCs was absent at 0.5 M, the value of k_s is calculated by $k_s = 8kT/3\eta$, where η is absolute viscosity of fluid. The calculated value of $T_{1/2}$ was 1.2 h, which was comparable to the time of injection of the MC suspension in phase 1 (i.e., 1.3 h). The calculations confirmed that aggregation of MCs could occur before attachment on sand surfaces.

To verify the existence of hydration cations during detachment, additional column experiments were conducted using the same experimental procedure as that adopted for Fig. 2. However, the concentration of Na^+ was determined instead of measuring colloid concentration using Inductively Coupled Plasma Optical Emission Spectrometer (ICP-OES) and an influent concentration of 100 mg L^{-1} for MC was used. We found that the mass recovery did not reach unity after flushing of DI water of phase 3. Specifically, the determined values of mass recovery for Na^+ were 94.5% and 97.1% with injection of 0.5 M and 0.1 M NaCl in phase 1, respectively. In contrast, the mass recoveries reached nearly unity if no MC was introduced in phase 1 (i.e., the control experiments). These results

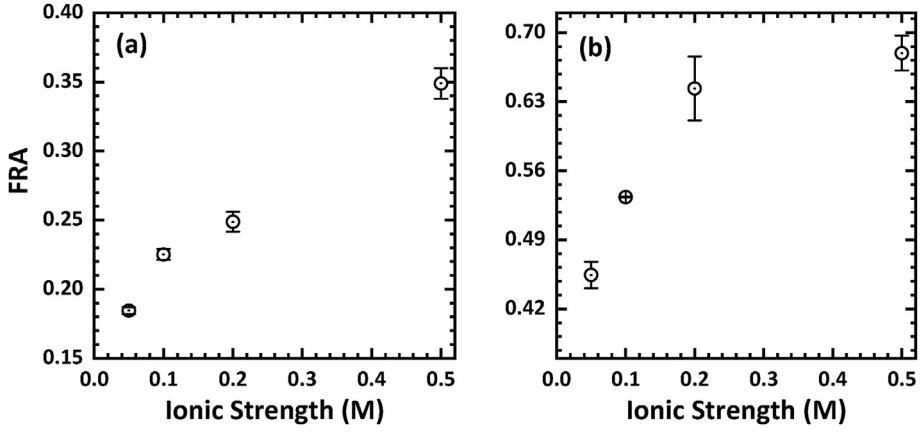

Fig. 4. Calculated value of FRA for the (a) NC and (b) MC as a function of IS of phase 1 for column transport experiments in Fig. 2.

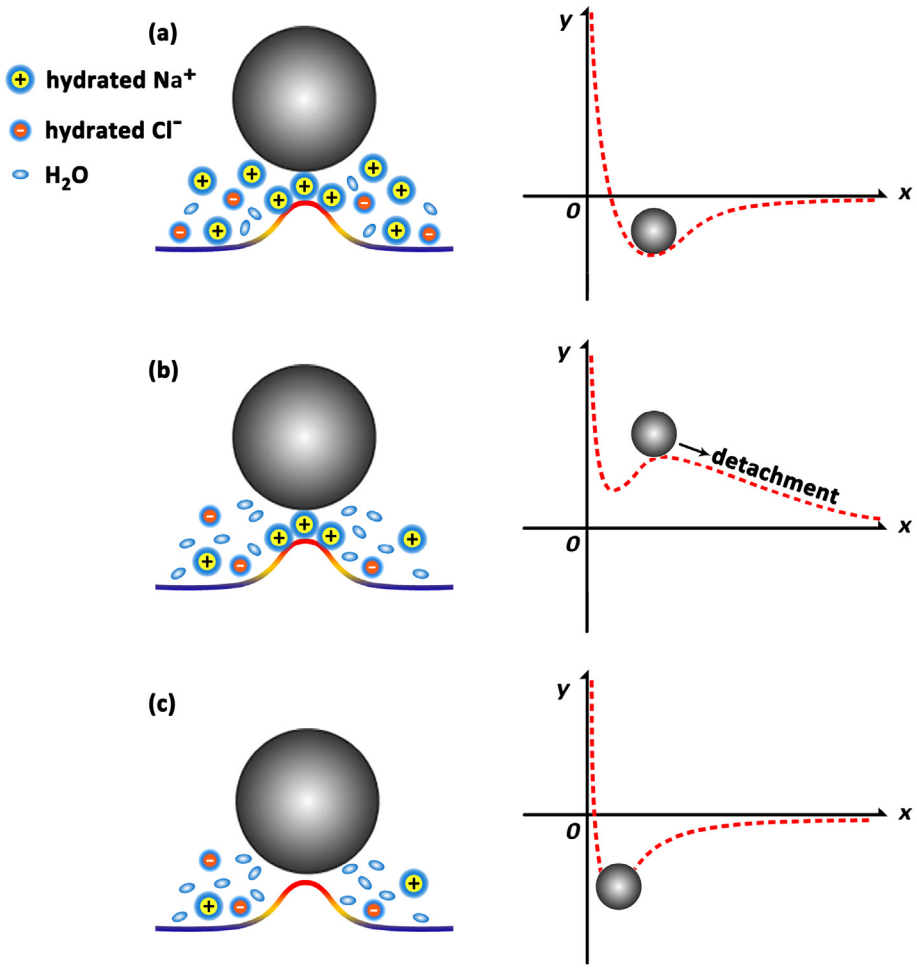

Fig. 5. Schematic illustration of influence of hydrated cations on attachment and detachment of a colloid in/from primary minima. (a), a colloid is attached in a shallow primary minimum atop a nanoscale protruding asperity at a large separation distance at a high IS due to hydrated cations between the colloid and asperity; (b), the hydrated cations remain in the gap between the colloid and protruding asperity when flushing DI water, and the colloid is detached from the shallow primary minimum due to repulsion; (c), hydration cations are displaced and the colloid is attached in a deeper primary minimum at a closer distance.

confirm the existence of hydration Na^+ cations during detachment and the interaction of the attached MC with the sand surfaces (e.g., at concave locations) play a critical role in remaining hydration cations.

It is worthwhile mentioning that the value of FRA should decrease with increasing IS when hydration repulsion is not considered. This is because colloids will be attached at deeper primary minima at a higher IS, and accordingly less colloids can be detached by an IS reduction, in contrast to the results in Fig. 4. Franchi and O'Melia (2003) showed the decrease of FRA with increasing solution IS by conducting column experiments using sulfate latex colloids and glass beads. They attributed the reason to the more dominance of irreversible attachment in primary minima over reversible attachment in secondary minima at a higher IS. The importance of hydration repulsion on colloid detachment from primary minima is verified by observations in Fig. 6. Specifically, additional NC and MC detachment can be achieved after completion of phase 3 by increasing the solution IS to 1 M NaCl (phase 4) and then flushing with DI water (phase 5). The elevation of the repulsive hydration force during phase 4 further weakened the adhesive interaction so that additional colloids can be released when the IS was reduced during phase 5. As mentioned above, solute equilibrium should not be reached in the gaps between the colloids and rough surfaces when flushing with DI water during phase 5 (c.f., Fig. 5b). This means that the rate of decrease of hydration with IS reduction is much slower than the rate of hydration increase with increasing IS (i.e., hydration hysteresis with IS). Conversely, if the rates of hydration were the same during IS increase (phase 4) and decrease (phase 5) then no additional colloids should be detached because there is no net change in hydration repulsion.

The elevation of hydration repulsion caused considerable in-situ clay release from soil in Fig. 7. In this case, a solution chemistry sequence of DI water, 1 M NaCl, and DI water was employed during phases 1, 2, and 3, respectively. The effluent clay concentration was monitored during this blank experiment. Details about the experimental procedure were shown in the SM. No clay release was observed during phases 1 and 2, whereas tremendous amounts of clay released occurred during phase 3. This detachment behavior in the soil occurs because of an increase in the repulsive hydration force when the IS was increased to 1 M NaCl during phase 2. Moreover, the high Na^+ concentration displaced multivalent cations such as Ca^{2+} and Mg^{2+} in the soil which can cause irreversible attachment by cation bridges (Schijven and Hassanizadeh, 2000; Bradford and Kim, 2010; Shen et al., 2012a; Torkzaban et al., 2013). The ICP-OES experiments confirmed the occurrence of cation exchange during phase 2 (see SM Fig. S10). Interestingly, the tails in the Na^+ breakthrough curves of SM Fig. S10 confirms the existence

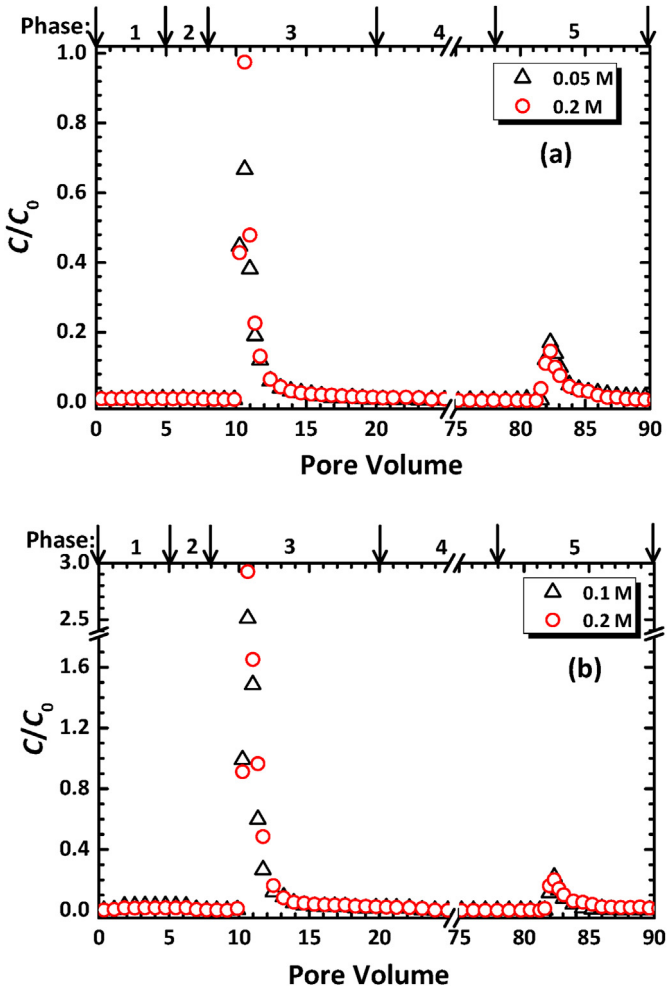

Fig. 6. Breakthrough curves for the (a) NC and (b) MC in sand columns. Phase 1, attachment of colloids at different ISs; Phase 2, elution with background NaCl electrolyte solution; Phase 3, elution with DI water; Phase 4, elution with 1 M NaCl electrolyte solution; Phase 5, elution with DI water.

of slow release of the Na^+ which caused the aforementioned hydration hysteresis. Note that no cation exchange was detected in the sand experiments of Figs. 2 and 4 due to thorough cleaning of the sand grains using the aggressive method of Zhuang et al. (2005) to remove multivalent cations that may exist on sand surfaces. In addition, no colloids were released in phase 2 when the IS was increased to 1 M because the increase of hydration by the IS increase cannot completely eliminate the primary minimum even at nanoscale protruding asperities. The interaction force was attractive at all separation distance under the favorable condition of 1 M NaCl, while the hydration is a short-range force, which only influences the interaction force at small separation distances.

3.4. Implications

The soil grains used in this study had been thoroughly washed and sonicated to remove clay colloids before packing the columns (see SM). Sonication has been commonly believed to be a very effective method for removal of colloidal particles from surfaces. However, numerous clay colloids were still detached from the sand after flushing the column with NaCl electrolyte solution with a high IS and then reducing the IS using DI water. Therefore, the use of high IS electrolyte solutions could be combined with other approaches (e.g., ultrasonic and megasonic methods) for enhancing surface cleaning that is critical to various industrial processes such as fabrication of semiconductors and microelectronic devices. However, elevating repulsive hydration forces with high IS salt solutions may also mobilize colloids that carry contaminants and enhance their transport in subsurface environments during IS reduction. Such colloid mobilization by hydration may be common in coastal zones where salinization and desalinization of groundwater are alternated. Therefore, accurate prediction of the transport and fate of contaminants in these areas should consider these factors.

4. Conclusions

Saturated column experiments were conducted to examine the role of hydration in the detachment of NCs and MCs in saturated sand porous media. Colloids were first attached in primary minima under high IS (NaCl) conditions, and a fraction of attached colloids were detached by introducing DI water to reduce the IS. DLVO interaction energy calculations and AFM examinations revealed that the detached colloids upon IS reduction were those initially attached atop of nanoscale protruding asperities on the sand surfaces where the primary minimum depth and adhesion were reduced. The FRA increased with the IS that the colloids were

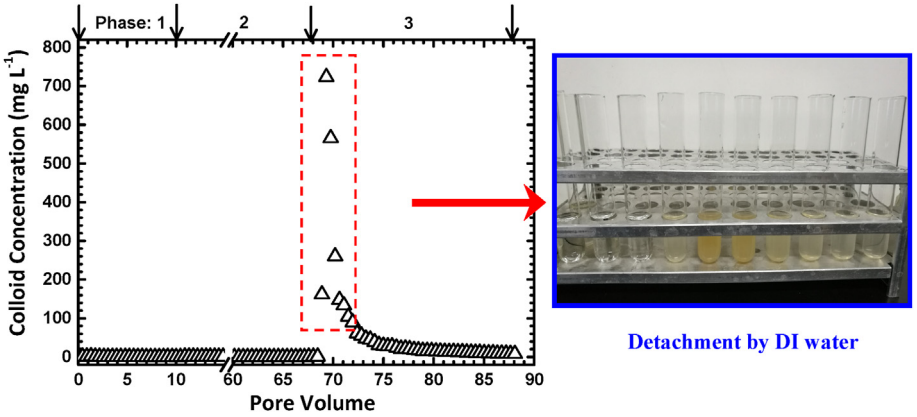

Fig. 7. The effluent concentration of clay colloids from soil columns as a function of pore volume. Phase 1, injection of DI water; Phase 2, elution with 1 M NaCl electrolyte solution; Phase 3, elution with DI water. The picture highlights that considerable clay colloids were detached with introducing DI water after using 1 M NaCl electrolyte solution to increase hydration repulsion. The clay colloid concentrations in the effluents were determined by measuring turbidities using UV−vis spectrophotometry at a wavelength of 680 nm.

initially attached because the hydration repulsion is larger at a higher IS and this causes colloids attached atop asperities to have weaker adhesions at farther distances. The weakly attached colloids are more readily detached by decreasing IS if the displacement of the cations between the colloids and asperities that causes hydration repulsion is retarded during the IS reduction. Our results suggest the importance of considering hydration in surface cleaning processes and in predicting the transport and fate of colloid-associated contaminants in areas such as coastal zones.

Declaration of competing interest

The authors declare that they have no known competing financial interests or personal relationships that could have appeared to influence the work reported in this paper.

Acknowledgments

We acknowledge the financial support provided by the National Natural Science Foundation of China (41671222, 41922047) and National Key Research and Development Program of China (2017YFD0800301).

Appendix A. Supplementary data

Supplementary data to this article can be found online at https://doi.org/10.1016/j.watres.2020.116068.

References

Alshibli, K.A., Alsaleh, M.I., 2004. Characterizing surface roughness and shape of sands using digital microscopy. J. Comput. Civ. Eng. 18, 36–45.
Anand, U., Lu, J., Loh, D., Aabdin, Z., Mirsaidov, U., 2016. Hydration layer-mediated pairwise interaction of nanoparticles. Nano Lett. 16 (1), 786–790.
Babakhani, P., Bridge, J., Doong, R., Phenrat, T., 2017. Continuum-based models and concepts for the transport of nanoparticles in saturated porous media: a state-of-the-science review. Adv. Colloid Interface Sci. 246, 75–104.
Batra, A., Paria, S., Manohar, C., Khilar, K.C., 2001. Removal of surface adhered particles by surfactants and fluid motions. AIChE J. 47 (11), 2557–2565.
Bedrikovetsky, P., Siqueira, F.D., Furtado, C.A., Souza, A.L.S., 2011. Modified particle detachment model for colloidal transport in porous media. Transport Porous Media 86 (2), 353–383.
Bergendahl, J., Grasso, D., 2000. Prediction of colloid detachment in a model porous media: Hydrodynamics. Chem. Eng. Sci. 55, 1523–1532.
Bhattacharjee, S., Elimelech, M., 1997. Surface element integration: a novel technique for evaluation of DLVO interaction between a particle and a flat plate. J. Colloid Interface Sci. 193, 273–285.
Bhattacharjee, S., Ko, C.-H., Elimelech, M., 1998. DLVO interaction between rough surfaces. Langmuir 14 (12), 3365–3375.
Bradford, S.A., Kim, H., 2010. Implications of cation exchange on clay release and colloid-facilitated transport in porous media. J. Environ. Qual. 39, 2040–2046.
Bradford, S.A., Torkzaban, S., 2015. Determining parameters and mechanisms of colloid retention and release in porous media. Langmuir 31, 12096–12105.
Bradford, S.A., Torkzaban, S., Leij, F., Simunek, J., 2015. Equilibrium and kinetic models for colloid release under transient solution chemistry conditions. J. Contam. Hydrol. 181, 141–152.
Bradford, S.A., Kim, H., Shen, C., Sasidharan, S., Shang, J., 2017. Contributions of nanoscale roughness to anomalous colloid retention and stability behavior. Langmuir 33 (38), 10094–10105.
Bradford, S.A., Sasidharan, S., Kim, H., Hwang, G., 2018. Comparison of types and amounts of nanoscale heterogeneity on bacteria retention. Front. Environ. Sci 6. https://doi.org/10.3389/fenvs.2018.0056.
Chen, S., Wang, F., Chu, W., Li, X., Wei, H., Gao, N., 2019. Weak magnetic field accelerates chloroacetamide removal by zero-valent iron in drinking water. Chem. Eng. J. 358, 40–47.
Crist, J.T., McCarthy, J.F., Zevi, Y., Baveye, P., Throop, J.A., Steenhuis, T.S., 2004. Pore-scale visualization of colloid transport and retention in partly saturated porous media. Vadose Zone J. 3, 444–450.
Elimelech, M., 1990. Indirect evidence for hydration forces in the deposition of polystyrene latex colloids on glass surfaces. J. Chem. Soc. Faraday. Trans. 86 (9), 1623–1624.
Elimelech, M., O'Melia, C.R., 1990. Kinetics of deposition of colloidal particles in porous media. Environ. Sci. Technol. 24 (10), 1528–1536.
Elimelech, M., Nagai, M., Ko, C.-H., Ryan, J.N., 2000. Relative insignificance of mineral grain zeta potential to colloid transport in geochemically heterogeneous porous media. Environ. Sci. Technol. 34 (11), 2143–2148.
Fang, B., Jiang, Y., Rotello, V.M., Nusslein, K., Santore, M.M., 2014. Easy come easy go: surfaces containing immobilized nanoparticles or isolated polycation chains facilitate removal of captured Staphylococcus aureus by retarding bacterial bond maturation. ACS Nano 8, 1180–1190.
Franchi, A., O'Melia, C.R., 2003. Effects of natural organic matter and solution chemistry on the deposition and reentrainment of colloids in porous media. Environ. Sci. Technol. 37, 1122–1129.
Grasso, D., Subramaniam, K., Butkus, M., Strevett, K., Bergendahl, J., 2002. A review of non-DLVO interactions in environmental colloidal systems. Rev. Environ. Sci. Biotechnol. 1 (1), 17–38.
Hahn, M.W., Abadzic, D., O'Melia, C.R., 2004. Aquasols: on the role of secondary minima. Environ. Sci. Technol. 38 (22), 5915–5924.
Hahn, M.W., O'Melia, C.R., 2004. Deposition and reentrainment of Brownian particles in porous media under unfavorable chemical conditions: Some concepts and applications. Environ. Sci. Technol. 38 (1), 210–220.
Hilpert, M., Rasmuson, A., Johnson, W.P., 2017. A binomial modeling approach for unscaling colloid transport under unfavorable conditions: Emergent prediction of extended tailing. Water Resour. Res. 53, 5626–5644.
Hong, H., Cai, X., Shen, L., Li, R., Lin, H., 2017. Membrane fouling in a submerged membrane bioreactor: new method and its applications in interfacial interaction quantification. Bioresour. Technol. 241, 406–414.
Israelachvili, J.N., Pashley, R.M., 1983. Molecular layering of water at surfaces and origin of repulsive hydration forces. Nature 306, 249–250.
Israelachvili, J., Wennerstrom, H., 1996. Role of hydration and water structure in biological and colloidal interactions. Nature 379, 219–225.
Israelachvili, J.N., 2010. Intermolecular and Surface Forces, 3 rd ed. Elsevier, Amsterdam.
Johnson, W.P., Li, X., Yal, G., 2007. Colloid retention in porous media: mechanistic confirmation of wedging and retention in zones of flow stagnation. Environ. Sci. Technol. 41, 1279–1287.
Johnson, W.P., Ma, H., Pazmino, E., 2011. Straining credibility: a general comment regarding common arguments used to infer straining as the mechanism of colloid retention in porous media. Environ. Sci. Technol. 45, 3831–3832.
Johnson, W.P., Rasmuson, A., Pazmino, E., Hilpert, M., 2018. Why variant colloid transport behaviors emerge among identical individuals in porous media when colloid-surface repulsion exists. Environ. Sci. Technol. 52, 7230–7239.
Kananizadeh, N., Peev, D., Delon, T., Schubert, E., Bartelt-Hunt, S., Schubert, M., Zhang, J., Uhlmann, P., Lederer, A., Li, Y., 2019. Visualization of label-free titanium dioxide nanoparticle deposition on surfaces with nanoscale roughness. Environ. Sci.: Nano. https://doi.org/10.1039/C8EN00984H.
Kang, S., Liu, S., Wang, H., Cai, W., 2016. Enhanced degradation performances of plate-like micro/nanostructured zero valent iron to DDT. J. Hazard Mater. 307, 145–153.
Kuznar, Z.A., Elimelech, M., 2007. Direct microscopic observation of particle deposition in porous media: role of the secondary energy minimum. Colloids Surf., A 294, 156–162.
Leng, Y., 2012. Hydration force between mica surfaces in aqueous KCl electrolyte solution. Langmuir 28 (12), 5339–5349.
Li, T., Jin, Y., Huang, Y., Li, B., Shen, C., 2017. Observed dependence of colloid detachment on the concentration of initially attached colloids and collector surface heterogeneity in porous media. Environ. Sci. Technol. 51 (5), 2811–2820.
Liang, Y., Hilal, N., Langston, P., Starov, V., 2007. Interaction forces between colloidal particles in liquid: theory and experiment. Adv. Colloid Interface 134–135, 151–166.
Lin, S., Wiesner, M.R., 2012. Deposition of aggregated nanoparticles-A theoretical and experimental study on the effect of aggregation state on the affinity between nanoparticles and a collector surface. Environ. Sci. Technol. 46, 13270–13277.
Logan, B.E., Jewett, D.G., Arnold, R.G., Bouwer, E.J., O'Melia, C.R., 1995a. Clarification of clean-bed filtration models. J. Environ. Eng. 121, 869–873.
Logan, B.E., Passow, U., Alldredge, A.L., Grossart, H.-P., Simon, M., 1995b. Rapid formation and sedimentation of large aggregates is predictable from coagulation rates (half-lives) of transparent exopolymer particles (TEP). Deep-Sea Res. II 42, 203–214.
Mahmood, T., Amirtharajah, A., Sturm, T.W., Dennett, K.E., 2001. A micromechanics approach for attachment and detachment of asymmetric colloidal particles. Colloids Surf., A 177, 99–110.
Manciu, M., Ruckenstein, E., 2001. Oscillatory and monotonic polarization. The polarization contribution to the hydration force. Langmuir 17 (24), 7582–7592.
Manciu, M., Ruckenstein, E., 2004. The polarization model for hydration/double layer interactions: the role of the electrolyte ions. Adv. Colloid Interface 112 (1-3), 109–128.
Miao, R., Wang, L., Mi, N., Gao, Z., Liu, T., Lv, Y., Wang, X., Meng, X., Yang, Y., 2015. Enhancement and mitigation mechanisms of protein fouling of ultrafiltration membranes under different ionic strengths. Environ. Sci. Technol. 49 (11), 6574–6580.
Miao, R., Wang, L., Zhu, M., Deng, D., Li, S., Wang, J., Liu, T., Lv, Y., 2017. Effect of hydration forces on protein fouling of ultrafiltration membranes: the role of protein charge, hydrated ion species, and membrane hydrophilicity. Environ. Sci. Technol. 51 (1), 167–174.
Molina-Bolívar, J.A., Ortega-Vinuesa, J.L., 1999. How proteins stabilize colloidal particles by means of hydration forces. Langmuir 15 (8), 2644–2653.
Molina-Bolıvar, J.A., Galisteo-González, F., Hidalgo-Alvarez, R., 2001. Specific cation

adsorption on protein-covered particles and its influence on colloidal stability. Colloids Surf., B 21 (1-3), 125–135.
Molnar, I.L., Johnson, W.P., Gerhard, J.I., Willson, C.S., O'Carroll, D.M., 2015a. Predicting colloid transport through saturated porous media: a critical review. Water Resour. Res. 51, 6804–6845.
Molnar, I.L., Gerhard, J.I., Willson, C.S., O'Carroll, D.M., 2015b. The impact of immobile zone on the transport and retention of nanoparticles in porous media. Water Resour. Res. 51, 8973–8994.
Ohki, S., Ohshima, H., 1999. Interaction and aggregation of lipid vesicles (DLVO theory versus modified DLVO theory). Colloids Surf., B 14 (1-4), 27–45.
Pashley, R.M., 1981. DLVO and hydration forces between mica surfaces in Li^+, Na^+, K^+, and Cs^+ electrolyte solutions: a correlation of double-layer and hydration forces with surface cation exchange properties. J. Colloid Interface Sci. 83 (2), 531–546.
Pashley, R.M., 1982. Hydration forces between mica surfaces in electrolyte solutions. Adv. Colloid Interface Sci. 16 (1), 57–62.
Pashley, R.M., Israelachvili, J.N., 1984. DLVO and hydration forces between mica surfaces in Mg^{2+}, Ca^{2+}, Sr^{2+}, and Ba^{2+} chloride solution. J. Colloid Interface Sci. 97 (2), 446–455.
Pazmino, E., Trauscht, J., Dame, B., Johnson, W.P., 2014. Power law size-distributed heterogeneity explains colloid retention on soda lime glass in the presence of energy barriers. Langmuir 30 (19), 5412–5421.
Rasmuson, A., VanNess, K., Ron, C.A., Johnson, W.P., 2019. Hydrodynamic versus surface interaction impacts of roughness inclosing the gap between favorable and unfavorable colloid transport conditions. Environ. Sci. Technol. 53, 2450–2459.
Ron, C.A., VanNess, K., Rasmuson, A., Johnson, W.P., 2019. How nanoscale surface heterogeneity impacts transport of nano- to micro-particles on surfaces under unfavorable attachment conditions. Environ. Sci. Nano 6, 1921–1931.
Ruckenstein, E., Manciu, M., 2003. Specific ion effects via ion hydration: II. Double layer interaction. Adv. Colloid Interface Sci. 105, 177–200.
Ryan, J.N., Elimelech, M., 1997. Colloid mobilization and transport in groundwater. Colloids Surf., A 107 (95), 1–56.
Santore, M.M., Kozlova, N., 2007. Micrometer scale adhesion on nanometer-scale patchy surfaces: adhesion rates, adhesion thresholds, and curvature-based selectivity. Langmuir 23 (9), 4782–4791.
Schijven, J.F., Hassanizadeh, M., 2000. Removal of viruses by soil passage: Overview of modeling, processes, and parameters. Crit. Rev. Environ. Sci. Technol. 30, 49–127.
Shen, C., Li, B., Huang, Y., Jin, Y., 2007. Kinetics of coupled primary- and secondary-minimum deposition of colloids under unfavorable chemical conditions. Environ. Sci. Technol. 41 (20), 6976–6982.
Shen, C., Lazouskaya, V., Jin, Y., Li, B., Ma, Z., Zheng, W., Huang, Y., 2012a. Coupled factors influencing detachment of nano- and micro-sized particles from primary minima. J. Contam. Hydrol. 134–135, 1–11.
Shen, C., Lazouskaya, V., Zhang, H., Wang, F., Li, B., Jin, Y., Huang, Y., 2012b. Theoretical and experimental investigation of detachment of colloids from rough collector surfaces. Colloids Surf. A 410, 98–110.
Shen, C., Lazouskaya, V., Zhang, H., Li, B., 2013. Influence of surface chemical heterogeneity on attachment and detachment of microparticles. Colloids Surf., A 433, 14–29.
Shen, C., Zhang, M., Zhang, S., Wang, Z., Zhang, H., Li, B., Huang, Y., 2015. Influence of surface heterogeneities on reversibility of fullerene (nC_{60}) nanoparticle attachment in saturated porous media. J. Hazard Mater. 290, 60–68.
Shen, C., Bradford, S.A., Li, T., Li, B., Huang, Y., 2018. Can nanoscale surface charge heterogeneity really explain colloid detachment from primary minima upon reduction of solution ionic strength? J. Nano Res. 20, 165,. https://doi.org/10.1007/s11051-018-4265-8.
Shen, C., Jin, Y., Zhuang, J., Li, T., Xing, B., 2020. Role and importance of surface heterogeneities in transport of particles in saturated porous media. Crit. Rev. Environ. Sci. Technol. 50, 244–329.
Shi, D., Zhu, G., Zhang, X., Zhang, X., Zhang, X., Li, X., Fan, J., 2018. Ultra-small and recyclable zero-valent iron nanoclusters for rapid and highly efficient catalytic reduction of p-nitrophenol in water. Nanoscale 11, 1000–1010. https://doi.org/10.1039/c8nr08302a.
Solovitch, N., Labille, J., Rose, J., Chaurand, P., Borschneck, D., Wiesner, M.R., Bottero, J.Y., 2010. Concurrent aggregation and deposition of TiO_2 nanoparticles in a sandy porous media. Environ. Sci. Technol. 44, 4897–4902.
Song, S., Peng, C., Olivares, M.A.G., Valdivieso, A.L., Fort, T., 2005. Study on hydration layers near nanoscale silica dispersed in aqueous solutions through viscosity measurement. J. Colloid Interface Sci. 287 (1), 114–120.
Song, Y., Fang, G., Zhu, C., Zhu, F., Wu, S., Chen, N., Wu, T., Wang, Y., Gao, I., Zhou, D., 2019. Zero-valent iron activated persulfate remediation of polycyclic aromatic hydrocarbon-contaminated soils: an in situ pilot-scale study. Chem. Eng. J. 355, 65–75.
Szilagyi, I., Szabo, T., Desert, A., Trefalt, G., Oncsik, T., Borkovec, M., 2014. Particle aggregation mechanisms in ionic liquids. Phys. Chem. Chem. Phys. 16, 9515–9524.
Tian, J., Jin, J., Chiu, P.C., Cha, D.K., Guo, M., Imhoff, P.T., 2019. A pilot-scale, bi-layer bioretention system with biochar and zero-valent iron for enhanced nitrate removal from stormwater. Water Res. 148, 378–387.
Torkzaban, S., Bradford, S.A., Wan, J., Tokunaga, T., Masoudih, A., 2013. Release of quantum dot nanoparticles in porous media: role of cation exchange and aging time. Environ. Sci. Technol. 47, 11528–11536.
Torkzaban, S., Bradford, S.A., 2016. Critical role of surface roughness on colloid retention and release in porous media. Water Res. 88, 274–284.
Tosco, T., Tiraferri, A., Sethi, R., 2009. Ionic strength dependent transport of microparticles in saturated porous media: modeling mobilization and immobilization phenomena under transient chemical conditions. Environ. Sci. Technol. 43 (12), 4425–4431.
Trauscht, J., Pazmino, E., Johnson, W.P., 2015. Prediction of nanoparticle and colloid attachment on unfavorable mineral surfaces using representative discrete heterogeneity. Langmuir 31 (34), 9366–9378.
Tufenkji, N., Elimelech, M., 2004. Correlation equation for predicting single collector efficiency in physicochemical filtration in saturated porous media. Environ. Sci. Technol. 38 (2), 529–536.
Tufenkji, N., Elimelech, M., 2005. Breakdown of colloid filtration theory: role of the secondary energy minimum and surface charge heterogeneities. Langmuir 21 (23), 841–852.
Vadillo-Rodriguez, V., Logan, B.E., 2006. Localized attraction correlates with bacterial adhesion to glass and metal oxide substrata. Environ. Sci. Technol. 40 (9), 2983–2988.
VanNess, K., Rasmuson, A., Ron, C.A., Johnson, W.P., 2019. A unified force and torque balance for colloid transport: predicting attachment and mobilization under favorable and unfavorable conditions. Langmuir 35, 9061–9070.
Verwey, E.J.W., Overbeek, J.ThG., 1948. Theory of the Stability of Lyophobic Colloids. Elsevier, Amsterdam.
Wang, H., Zhang, W., Zeng, S., Shen, C., Jin, C., Huang, Y., 2019. Interactions between nanoparticles and fractal surfaces. Water Res. 151, 296–309.
Wang, Z., Wang, D., Li, B., Wang, J., Li, T., Zhang, M., Huang, Y., Shen, C., 2016a. Detachment of fullerene nC60 nanoparticles in saturated porous media under flow/stop-flow conditions: column experiments and mechanistic explanations. Environ. Pollut. 213, 698–709.
Wang, Z., Jin, Y., Shen, C., Li, T., Huang, Y., Li, B., 2016b. Spontaneous detachment of colloids from primary minima by Brownian diffusion. PLoS ONE 11, e0147368. https://doi.org/10.1037/journal.pone.0147368.
Xu, S., Qi, J., Chen, X., Lazouskaya, V., Zhuang, J., Jin, Y., 2016. Coupled effect of extended DLVO and capillary interactions on the retention and transport of colloids through unsaturated porous media. Sci. Total Environ. 573, 564–572.
Yao, K., Habibian, M.T., O'Melia, C.R., 1971. Water and waste water filtration: concepts and applications. Environ. Sci. Technol. 5 (11), 1105–1112.
Yu, C., Ma, J., Zhang, J., Lou, J., Wen, D., Li, Q., 2014. Modulating particle adhesion with micro-patterned surfaces. ACS Appl. Mater. Interfaces 6, 8199–8207.
Zhao, L., Zhang, M., He, Y., Chen, J., Hong, H., Liao, B.-Q., Lin, H., 2016. A new method for modeling rough membrane surface and calculation of interfacial interactions. Bioresour. Technol. 200, 451–457.
Zhou, D., Wang, D., Cang, L., Hao, X., Chu, L., 2011. Transport and re-entrainment of soil colloids in saturated packed column: effects of pH and ionic strength. J. Soil Sed 11 (3), 491e503.
Zhuang, J., Qi, J., Jin, Y., 2005. Retention and transport of amphiphilic colloids under unsaturated flow conditions: effect of particle size and surface property. Environ. Sci. Technol. 39 (20), 7853–7859.
Zou, Y., Jayasuriya, S., Manke, C.W., Mao, G., 2015. Influence of nanoscale surface roughness on colloidal force measurements. Langmuir 31 (38), 10341–10350.